

# Detection of Pigment Networks in Dermoscopy Images

**Khalid Eltayef, Yongmin Li and Xiaohui Liu**

Computer Science Department, Brunel University London, Uxbridge, UB8 3PH, UK

E-mail: [khalid.eltayef@Brunel.ac.uk](mailto:khalid.eltayef@Brunel.ac.uk), [Yongmin.Li@Brunel.ac.uk](mailto:Yongmin.Li@Brunel.ac.uk),  
[XiaoHui.Liu@brunel.ac.uk](mailto:XiaoHui.Liu@brunel.ac.uk)

**Abstract.** One of the most important structures in dermoscopy images is the pigment network, which is also one of the most challenging and fundamental task for dermatologists in early detection of melanoma. This paper presents an automatic system to detect pigment network from dermoscopy images. The design of the proposed algorithm consists of four stages. First, a preprocessing algorithm is carried out in order to remove the noise and improve the quality of the image. Second, a bank of directional filters and morphological connected component analysis are applied to detect the pigment networks. Third, features are extracted from the detected image, which can be used in the subsequent stage. Fourth, the classification process is performed by applying feed-forward neural network, in order to classify the region as either normal or abnormal skin. The method was tested on a dataset of 200 dermoscopy images from Hospital Pedro Hispano (Matosinhos), and better results were produced compared to previous studies.

**Keywords.** Dermoscopy image, pigment network detection, directional filters, features extraction.

## 1. Introduction

Malignant melanoma is the most frequent type of skin cancer and the detection of the early stage is a challenging and fundamental task for dermatologists, with the early diagnosis, the patients probability of survival increases greatly. Dermoscopy is a widely common technique used to perform an in-vivo observation of pigmented skin lesions.[1].

The pigment network is one of the most relevant dermoscopic structures for its appearance on the body is an indicator of the existence of melanin in deep layers of the skin. The shape of the pigment network can be classified as either Typical or Atypical: typical when the pattern is regularly with a light-to-dark-brown network small uniform space network holes and thin network lines distributed more or less regular throughout the lesion, while atypical is characterized by black, brown, or gray and thickened lines distributed more or less irregularly throughout the lesion. Therefore, an atypical pigment network signals a melanoma[2][3].

Computer Aided Diagnosis (CAD) systems have been proposed by many different groups to identify malignant melanomas in dermoscopy images. These systems use several features, such as color, shape and texture, to classify the images as either normal or abnormal. [2][3][4]. In the detection of melanoma dermatologists use the ABCD rule to analyze four parameters (Asymmetry, Border, Colors and Diameter) and distinguish skin lesions or the 7-points checklist which is a scoring method for a set of different classify depending on color, shape and texture

[5][4].

An automatic detection of pigment networks is a challenging task, because there is a smooth transition between the color of the pigment network lines and the background. Moreover, presence of dark hair covering the lesions and the existence of specular reflection. In addition, the circular structures such as dots are detected as pigment networks wrongly, or vice-versa [3]. In this paper, four steps have been performed to implement an automatic algorithm for the detection of pigment networks in dermoscopy images. First, the image is pre-processed in order to remove artifacts such as hairs and reflection detection. Second, based on the intensity values and geometrical properties of the pigment networks, a set of tentative pigment network regions are detected. Then, features are extracted from the given lesion and by using a trained classifier, the given lesion is classified in one of two classes (with or without pigment network). The paper is structured as follows. Section 2 provides an overview of the method developed previously. The proposed system is described in details in sections 3-6. The evaluation and the performance of the detection system and the results obtained are discussed in Sections 7. Finally, conclusions are presented in section 8.

## 2. Previous Work

Sadeghi et al.[6] aim to detect the holes of the network. Three different stages were implemented to detect the holes, first a Laplacian of Gaussian (LoG) filter is used in order to find meshes or cyclic structures. Second, an 8-connected components analysis is applied to transform the filtered image to a set of graphs. Finally, a search for loops or cyclic graphs is carried out. Then the distance between the holes is measured and based on this distance a new graph is created. This graph is used for the detection of pigment network. The same research group presented a new method for classification between Absent, Typical and Atypical [7]. They detected the net structure and extracted structural, geometric, chromatic and texture features, and then they used these features to train a boosting classifier. Two different techniques structural and spectral are proposed by Betta et al.[8] They started to combine these techniques to perform the detection of pigment network. Firstly, they used structural techniques to search for simple shape structures, like lines or dots. Secondly, the spectral technique is based on a Fourier analysis of gray-level image. A sequence of Fast Fourier Transform, high-pass filtering, Inverse Fast Fourier Transform and thresholding were applied. Eventually, the mask from each technique is combined together to provide a network image. This study has been updated and proposed by Di Leo et al.[9] They classified the areas which constitute the network image as either atypical or typical, the existence of typical pigment network or the absence of network are both included in the same class. Chromatic and spatial features such as mean and standard deviation related to the obtained structures were extracted, and used to train a decision tree algorithm.

Grana et al.[10] Proposed an algorithm to undertake the detection of the pigment network. They used Gaussian derivative kernel to detect the net edges and Fisher linear technique to provide the optimal thresholds. Morphological masks are used to complete the line linking process. However, the experiments which has been performed are not focused on the task of distinguish between pigment network and no pigment network.

Barata et al.[3] proposed an algorithm to detect pigment networks using a bank of direction filters and morphological operations. They used two distinctive properties, region pigment network intensity and geometry, features were extracted and an Adaboost algorithm was used to classify the region as either with or without pigment network (normal or abnormal skin).

## 3. Pre-processing

The purpose of image pre-processing is to improve the image data by removing unwanted distortions from the image or enhancing image features, which can be used as input to other image processing techniques. Pre-processing is an important step in medical image analysis, in

order to avoid affecting the extraction of the object by noise, and it facilitates the segmentation process. In dermoscopy images, two main kinds of noise must be removed before doing any step, hairs and reflection artifacts caused by placing gel or oil before capturing the image. Incorrect segmentation of pigment network can be extracted if hairs covering the image are not removed, since hair shapes are similar to pigment network lines. Consequently, the classification of the given region may be incorrect. This process involves two key operations: hairs, reflection artifact detections and removal. The original RGB images were separated to three color components, and the blue component is selected for its best discriminative capacity[11].

### 3.1. Reflection detection

Reflection artifacts and air bubbles appear like noise in dermoscopy images due to placement of oil or gel on the lesion area before capturing the image. To detect this kind of noise, a simple threshold algorithm is applied. Every single pixel  $(x, y)$  can be detected and classified as a reflection artifact if its intensity value is higher than threshold  $T_{R1}$  and if its intensity value minus the average intensity  $I_{avg}(x, y)$  of its surrounding neighborhood is higher than threshold  $T_{R2}$ , *i.e.*

$$\{I(x, y) > T_{R1}\} \text{ and } \{(I(x, y) - I_{avg}(x, y)) > T_{R2}\}. \quad (1)$$

where  $I$  is the image,  $I_{avg}(x, y)$  is the average intensity value in a local neighborhood of the selected pixel which is computed using a local mean filter with dimensions 11x11 and  $T_{R1}=0.7$ ,  $T_{R2}=0.098$ .

### 3.2. Hair detection

Due to the similarity between hairs and pigment networks in dermoscopy images, it is challenging to detect hairs without any effect of the pigment networks. This similarity may lead to incorrect detection and decrease in classification accuracy since the shape of the hairs similar to the shape of the pigment networks. Then, the same algorithm can be used to detect both. Directional Gabor filters are implemented to extract hair artifacts and pigment networks from dermoscopy images. However, the parameters used in the Gaussian filters at each stage are different [3]. A bank of 64 directional filters has been used to perform hair detection. Let

$$h\theta_i(x, y) = G_1(x, y) - G_2(x, y). \quad (2)$$

be the impulse of a directional filter with angle  $\theta_i$  where  $\theta_i \in [0, \pi]$ ,  $i=0 \cdots 64$  and  $G_k$  is a Gaussian filter:

$$G_K(x, y) = C_K \exp\left\{-\frac{x'^2}{2\sigma_{x_k}^2} - \frac{y'^2}{2\sigma_{y_k}^2}\right\}, k = 1, 2. \quad (3)$$

The difference between two consecutive filters  $\theta_i$  and  $\theta_{i+1}$  is constant and equal to  $\frac{\pi}{N}$ . Therefore,  $N + 1$  filter are used. In (3),  $C_K$  is a normalization constant and the values of  $(x', y')$  are dependent on or related with  $(x, y)$  by a rotation of amplitude  $\theta_i$ .

$$x' = x \cos \theta_i + y \sin \theta_i. \quad (4a)$$

$$y' = y \cos \theta_i - x \sin \theta_i. \quad (4b)$$

Parameters value have been experimentally obtained and set as:  $\sigma_{x1}=20$ ,  $\sigma_{y1}=6$ ,  $\sigma_{x2}=20$  and  $\sigma_{y2}=0.5$ . The size of the mask filter is 41 x 41.

The difference of Gaussians in Equation (2) is used since it allows a better enhancement of directional structures while removing the effect of the background. The image  $I$  is filtered

by each directional filter. The output of the  $i$ th directional filter is given by the following convolution:

$$I_i(x, y) = h\theta_i(x, y) * I(x, y). \quad (5)$$

After filtering the image by each directional filter, the combination of the output of  $N + 1$  directional filters are estimated and the maximum output at each pixel  $(x, y)$  is selected according to the following equation.

$$J(x, y) = \max_{i \in \{1, 2, \dots, N+1\}} (I_i(x, y)). \quad (6)$$

where  $J$  is the final image obtained from Gabor filter, this image contains both: hairs and pigment network lines. Adjusting the threshold is tricky. Therefore, we used a different approach and produced better results. Image sharpening is applied on the outcome image from Gabor filter, to increase the contrast between different colors, and sharpen the transition from black to white, where all edges become sharp. Then, Sobel filter is applied on the sharpened image with threshold of 0.0145, this process ignores all edges that are not stronger than the threshold value, and detect the rest of the edges as hair. In this case, every single hair is detected and classified as a noise. Therefore, many hairs were not classified in the previous method “Barata’s method” are detected and classified. Examples are illustrated in figure 1.

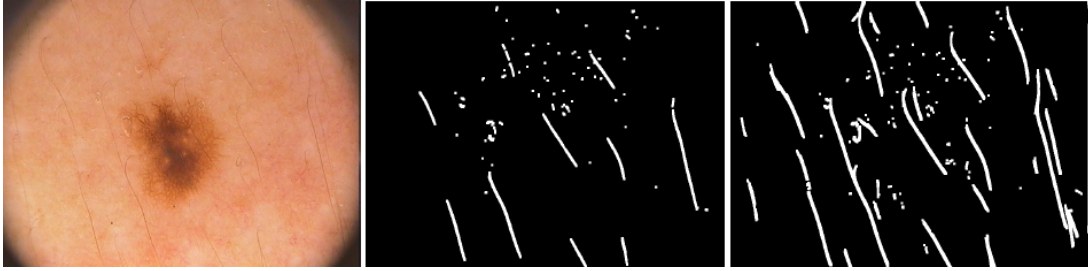


Figure 1: Examples of hair detection process: Original (first column), Barata’s method (second column) and our method (third column).

After reflection artifacts and hairs are detected, their binary masks are multiplied by gray scale image  $I(x, y)$ . This operation leads to appearance of gaps which can be filled by propagating the information from known region which it is the neighborhood into the unknown region [12].

#### 4. Pigment network detection

Pigment network and hair artifacts both have very similar line shape, and they appear with more than one orientation in dermoscopy images. Therefore, the same technique with different parameters can be used to detect the pigment networks from the dermoscopy images. Two main steps have been applied to do so: network enhancement and network detection. First, the output image that was obtained from pre-processing stage is filtered with a bank of directional filters [see (2)-(6)]. Due to the difference of the length and the width of each line stroke of the hairs and pigment network, the parameters used to detect the pigment networks are different from those used to detect the hairs. These parameters were set as:  $\sigma_{x1}=40$ ,  $\sigma_{y1}=40$ ,  $\sigma_{x2}=3$  and  $\sigma_{y2}=0.5$  with mask filter dimension of 11 x 11 and  $T_H=0.0185$ . Then, to detect the pixels which belong to the net of pigment networks, a threshold value is implemented. The second step is to extracting large linked lines of pigment networks, since it is assumed that the pigment networks consists a set of connected lines. A connected component analysis can be used to identify the connectivity between the pixels. Eight-connectivity criterion is used because it provides the information of vertical, horizontal, and diagonals connections. A threshold value is applied for

each connected components, each connected component in the binary image is extracted and classified as a pigment network if its area is greater than threshold value, and it is given by following condition.

$$A(R_c) > A_{min} \quad (7)$$

where  $R_c$  is the  $c$ th connected region,  $A(R_c)$  is its area, and  $A_{min}$  is a threshold value which was set as 900 in our experiments. By applying the previous condition, all connected components with small area can be classified as noise. An example of pigment network detection is shown in figure 2. The obtained image is a binary “net mask ” of all connected regions according to following equation:

$$R = \bigcup_{c:A(R_c)>A_{min}} R_c \quad (8)$$

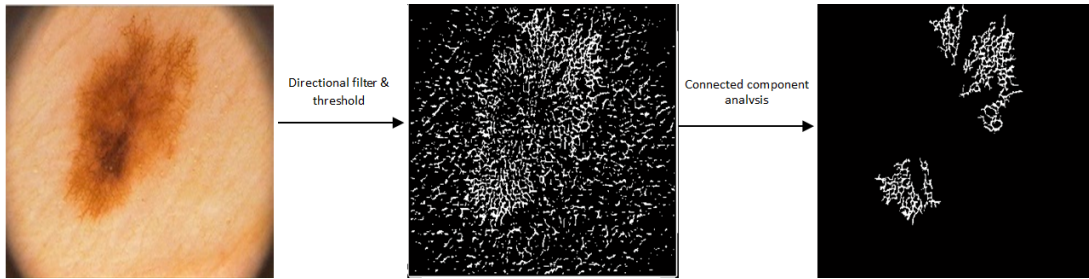


Figure 2: Example of pigment network detection

## 5. Feature extraction

The third stage of the proposed algorithm aims to extract the relevant features from the final binary images. The density and the regular distribution of the pigment networks are the main properties, and they can be used to identify the images where pigment network is present. By characterizing these two properties of pigment network, five features were defined:

**Network/Lesion Ratio:** This value computes the area of the network  $R$  (see section 4) with the area of the whole lesion

$$Network/Lesion = \frac{A(R)}{A(L)} \quad (9)$$

where  $A(R)$  is the area of the detected pigment network and  $A(L)$  is the area of the segmented lesion which has been segmented by an experienced dermatologist.

**Network/Region Ratio:** This value computes the area of the pigment network lines with the area of pigment network regions, because the pigment network consists of holes surrounded by pigmented lines. A simple morphological filling process is applied for all connected regions to get the pigment network region  $B_c$  (see Fig.3(c)). Then a pigment network regions mask is defined as the union of all the regions.

$$B = \cup_c B_c \quad (10)$$

The network/regions ratio is then obtained as following:

$$Network/Region = \frac{A(R)}{A(B)} \quad (11)$$

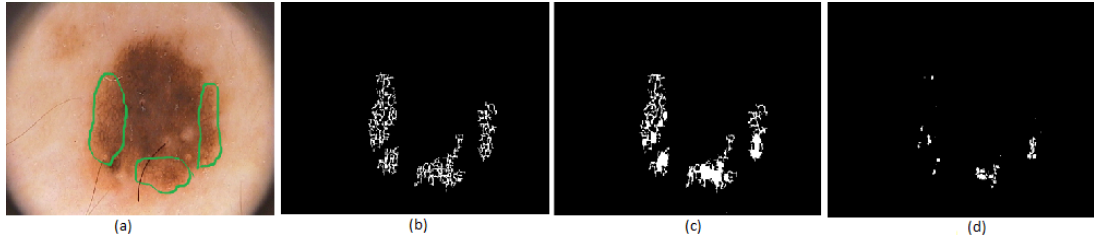


Figure 3: Pigment network masks. (a) original image with pigment network regions highlighted; (b) pigment network detection ;(c) pigment network regions-mask and (d) holes mask.

where  $A(R)$  is the area of the detected network  $R$  and  $A(B)$  is the area of all the pigment network regions present in  $B$ .

**Number Of Holes:** As above mentioned, the pigment network consists of holes surrounded by pigment network lines. Therefore, this value computes the total number of the holes of the detected net, it can be simply obtained by subtract  $R$  from  $B$ . Where  $R$  is the detected image and  $B$  is the union of all regions. An example can be seen on figure 3(d).

**Holes/Lesion Ratio:** This value compares the number of the holes with the area of the lesion.

$$Holes/lesion = \frac{H_n}{A(L)} \quad (12)$$

where  $H_n$  is the total number of the holes in the detected image and  $A(L)$  is the area of the segmented lesion  $L$ .

**Holes/Region Ratio:** This value compares the number of the holes with the area of the detected region.

$$Holes/Region = \frac{H_n}{A(B)} \quad (13)$$

where  $H_n$  is the total number of the holes in the detected image and  $A(B)$  is the area of all the pigment network regions  $B$ .

## 6. Lesion classification

The final stage of the proposed approach aims to determine the images type, using a machine learning technique. The five features extracted from previous step are used to feed an Artificial Neural Network (ANN) as a binary classifier. As a target: **(0)** indicates an abnormal skin and **(1)** indicates a normal skin. A two-layer feed-forward network (hidden layer and output layer) are used with 10 neurons in hidden layer, and scaled conjugate gradient backpropagation with sigmoid function are used to train the network.

## 7. Experimental results

The proposed approach was tested on a dataset of 200 dermoscopy images (84 with pigment network and 116 without pigment network) from the database of Hospital Pedro Hispano, Matosinhos. The images are labelled with two classes: melanoma and non-melanoma. We evaluate the performance using mean square error and confusion matrices. Quantitative comparison between various methods is difficult because different datasets and criteria have been used. We have evaluated our method against Barata et al [3] as they have the same objectives and they are based on the same dataset. Table 1 shows the comparison result. It indicates that our method by using Sobel filter after applying Gabor filter on the image to extract almost all hairs achieved better results and outperforms Barata et al. [3] by three criteria namely: sensitivity, specificity and accuracy. With a note that the results presented in table 1 are obtained by

Table 1: Results of the lesion classification SE-sensitivity, SP-specificity and AC-accuracy.

Work	SE	SP	AC
Barata et al	91.1%	82.1%	86.2%
Proposed method	92.3%	95.0%	90.0%

repeating neural network pattern recognition tool 20 times and obtaining the average in all the above mentioned criteria. Our proposed method successfully classified the given image as either normal or abnormal skin, as well as located the pigment network in dermoscopy images which can assist dermatologists in visual diagnosis and making right diagnosis decisions.

## 8. Conclusion

An approach of detection of pigment networks from dermoscopy images has been described. Gabor filter is combined with Sobel filter to perform hairs detection, and Barata's method has been used to extract pigment networks from dermoscopy images. The features extracted from the detected images are used to train a feed-forward neural network classifier. The proposed algorithm successfully achieved 92.3% sensitivity, 95.0% specificity and 90.0% classification accuracy.

## Acknowledgment

The database used in this study was acquired by Teresa Mendonc, Pedro M. Ferreira, Jorge S. Marques, Andre R. S. Marçal, and Jorge Rozeira from Pedro Hispano Hospital. The authors wish to thank Catarina Barata for sharing.

## References

- [1] [dermoscopy.org/atlas/base.htm](http://dermoscopy.org/atlas/base.htm)
- [2] Arroyo J L G and Zapirain B G 2014 *Computers in biology and medicine* **44** 144–157
- [3] Barata C, Marques J S and Rozeira J 2012 *Biomedical Engineering, IEEE Transactions on* **59** 2744–2754
- [4] Messadi M, Cherifi H and Bessaid A 2014 *Journal of Convergence Information Technology* **9** 21
- [5] Walter F M, Prevost A T, Vasconcelos J, Hall P N, Burrows N P, Morris H C, Kinmonth A L and Emery J D 2013 *Br J Gen Pract* **63** e345–e353
- [6] Sadeghi M, Razmara M, Lee T K and Atkins M S 2011 *Computerized Medical Imaging and Graphics* **35** 137–143
- [7] Sadeghi M, Razmara M, Wighton P, Lee T K and Atkins M S 2010 Modeling the dermoscopic structure pigment network using a clinically inspired feature set *Medical Imaging and Augmented Reality* (Springer) pp 467–474
- [8] Betta G, Di Leo G, Fabbrocini G, Paolillo A and Sommella P 2006 Dermoscopic image-analysis system: estimation of atypical pigment network and atypical vascular pattern *Medical Measurement and Applications, 2006. MeMea 2006. IEEE International Workshop on* (IEEE) pp 63–67
- [9] Di Leo G, Liguori C, Paolillo A and Sommella P 2008 An improved procedure for the automatic detection of dermoscopic structures in digital elm images of skin lesions *Virtual Environments, Human-Computer Interfaces and Measurement Systems, 2008. VECIMS 2008. IEEE Conference on* (IEEE) pp 190–194
- [10] Grana C, Cucchiara R, Pellacani G and Seidenari S 2006
- [11] Silveira M, Nascimento J C, Marques J S, Marçal A R, Mendonça T, Yamauchi S, Maeda J and Rozeira J 2009 *Selected Topics in Signal Processing, IEEE Journal of* **3** 35–45
- [12] Criminisi A, Perez P and Toyama K 2003 Object removal by exemplar-based inpainting *Computer Vision and Pattern Recognition, 2003. Proceedings. 2003 IEEE Computer Society Conference on* vol 2 (IEEE) pp II–721